Microstructure and mechanical properties of liquid-phase-sintered SiC + Si_3N_4 composites

A.Vysocká[1]*, J. Špaková[1], J. Dusza[1], M. Balog[2], P. Šajgalík[2]

[1] *Institute of Materials Research, SAS, Watsonova 47, 043 53 Košice, Slovak Republic*
[2] *Institute of Inorganic Chemistry, SAS, Dúbravská cesta 9, 845 36 Bratislava 45, Slovak Republic*

Received 29 March 2007, received in revised form 17 May 2007, accepted 8 June 2007

Abstract

The microstructure and some mechanical properties (Young's modulus, hardness, fracture toughness, and flexural strength) of as-received and heat-treated liquid-phase-sintered SiC + Si_3N_4 composites have been investigated. The hardness and the fracture toughness were determined by Vickers indentation method and the Young's modulus was measured by depth-sensing indentation test. Flexural strength measurement was performed by means of four-point bend test. The characteristic flexural strength and Weibull modulus were computed using two-parameter Weibull distribution. Fractographic analysis of broken flexural specimens was used to characterize the fracture initiation origins. The strength of the investigated materials was degraded by the present processing flaws in the form of pores and clusters of pores. The fracture toughness was enhanced by changing the SiC grains size and aspect ratio after the heat treatment at 1850 °C/5 h.

K e y w o r d s: SiC + Si_3N_4 composites, microstructure, flexural strength, Vickers hardness, indentation fracture toughness

1. Introduction

Silicon carbide and silicon nitride have been recognized as an important structural ceramics because of their good combination of thermal and mechanical properties. Si_3N_4 ceramics exhibit high fracture toughness and good flexural strength, but possess lower resistance to oxidation at high temperatures. On the contrary, SiC ceramics show good wear, creep and oxidation resistance at high temperatures, but low fracture toughness [1]. SiC is a promising material for high temperature applications, however, it is difficult to densify it without sintering additives because of the covalent nature of Si-C bonding and low self-diffusion coefficient. Prochazka [2] showed how to pressureless sinter SiC with B and C additives, allowing its use in a wide variety of applications requiring excellent wear and corrosion resistance. The main disadvantage of this solid-state-sintered material (SSiC) is the low fracture toughness (around 2.5 MPa $m^{1/2}$). For mechanically loaded structural applications, favourable properties may be expected especially in liquid-phase-sintered material (LPS-SiC). Compared to SSiC, very homogeneous and fine-grained microstructures can be obtained due to lower sintering temperatures and the presence of the liquid phase [3]. For dense bulk non-oxide ceramic materials various sintering additives have been reported such as Al_2O_3, Al_2O_3-Y_2O_3, yttrium-aluminium garnet (YAG), AlN-Y_2O_3 [4–9]. Silicon carbide compacts with Al_2O_3-Y_2O_3 could be sintered at low temperature due to the formation of a liquid phase by reaction between Al_2O_3, Y_2O_3 and SiC. The resulted material exhibits usually small grain size, which could be controlled by microstructure design through heat treatment after sintering.

The mechanical properties of LPS-SiC are strongly affected by its microstructure [10, 11]. The metastable β-SiC transforms at higher temperatures (around 2000 °C) to one of the α-SiC polytypes. This phase transformation has been applied to control the microstructure of liquid-phase-sintered SiC ceramics [12, 13]. The phase transformation from β-SiC to α-SiC has been reported to result in coarse elongated SiC

*Corresponding author: tel.: +421 55 792 2465; fax: +421 55 792 2408; e-mail address: avysocka@imr.saske.sk

Table 1. Chemical composition and heat treatment regimes of the investigated composites

Sample designation	Chemical composition (wt.%)				Heat treatment
	SiC	Si_3N_4	Y_2O_3	Al_2O_3	
SC-N-G5	86.5	5	5.7	2.8	HP: 1870 ℃/1 h
SC-N-A5	86.5	5	5.7	2.8	HP: 1870 ℃/1 h + AN: 1650 ℃/5 h
SC-N-B5	86.5	5	5.7	2.8	HP: 1870 ℃/1 h + AN: 1850 ℃/5 h

grains which offers an opportunity for an "in situ" reinforcement resulting in the increased toughness of SiC [3, 10, 14, 15]. Large elongated grains are the sources of the fracture toughness improvement through different toughening mechanisms, mainly the crack bridging [14, 16, 17] and/or crack deflection [4]. Although fracture toughness increases with an increase of transformed β-α SiC fraction, an opposite trend is observed in strength [18]. Zhou et al. [19] observed that the fracture toughness of SiC ceramics strongly depended on additive compositions in the Re_2O_3-Al_2O_3 system (Re = Y, La, Nd, Yb). To improve the toughness and high-temperature strength of LPS SiC ceramics, several combinations of additives, such as Al_2O_3, Y_2O_3, CaO, MgO, AlN, and, recently, rare-earth oxides have been investigated [20–23].

The aim of the present investigation is to study the influence of the microstructure of liquid phase sintered and heat treated SiC + Si_3N_4 composites on their mechanical properties, namely Young's modulus, Vickers hardness, indentation fracture toughness, and flexural strength.

2. Experimental procedure

Commercially available β-SiC powder (HSC-059, Superior Graphite), Si_3N_4 (AIY-3/54, Grade C, Plasma & Ceramic Technologies Ltd.), Al_2O_3 (A 16 SG, Alcoa), and Y_2O_3 (grade C, H. C. Starck) were used as the starting powders. The Si_3N_4 powder contains Y_2O_3 and Al_2O_3 as sintering additives in weight ratio 6 : 3. The powder mixtures were ball milled in isopropanol with SiC balls for 24 hours. The suspensions were dried, subsequently sieved through 25 μm sieve screen in order to avoid hard agglomerates. The samples were hot pressed at 1870 ℃/1 h under mechanical pressure of 30 MPa in N_2 atmosphere. Hot pressed samples were subsequently annealed under various time/temperature conditions given in Table 1. After sintering and annealing the specimens were cut, polished up to 1 μm finish, and etched using a boiling Murakami solution (10 g KOH + 10 g $K_3Fe(CN)_6$ + 100 ml H_2O) for 5–10 min.

The density was measured by Archimedes method in water. The phase identification of the sintered samples was performed by means of X-ray diffractometry (Philips X'Pert Pro) using Cu Kα radiation. The microstructures of polished and chemically etched specimens were studied using scanning electron microscopy (JEOL JSM-7000F) and applying transmission electron microscopy (JEM 2010). Image analysis was used to investigate SEM micrographs. The size of each grain (d) was directly obtained from the shortest diagonal of the grain in its two-dimensional image. The apparent length of grain (L) was determined from the longest diagonal. For TEM examination, discs with a diameter of 3 mm were cut from the bulk materials and mechanically ground to a thickness of 60 μm. They were further thinned to about 20 μm by dimpling, followed by Ar-ion thinning until perforation.

Vickers macro-/microhardness was measured at loads in an interval from 0.98 N to 98.1 N by using hardness testers (LECO 700AT, HPO 250). Indentation Young's modulus was estimated by depth-sensing method using a Vickers indenter (Fisherscope H 100) at load of 0.98 N. The fracture toughness was determined using an indentation method. The indents were introduced to the samples after polishing the surface to a 1 μm finish. At least 10 Vickers indentations per specimen were introduced with loads from 9.81 N to 147.15 N. The fracture toughness was calculated from the lengths of edge cracks and indentation diagonals using a formula valid for semi-circular crack systems as proposed by Anstis et al. [24]:

$$K_{IC} = 0.016 \left(\frac{E}{H}\right)^{1/2} \left(\frac{P}{c^{3/2}}\right), \qquad (1)$$

where K_{IC} is fracture toughness (MPa $m^{1/2}$); 0.016 is material-independent constant for Vickers-produced radial cracks; E is Young's modulus (GPa); H is Vickers hardness (GPa); P is indentation load (N); c is half-length of the radial crack (m).

The strength was measured using specimens with dimensions 3 × 4 × 45 mm, tested in four point bending mode. They were ground and polished by 15 μm diamond grinding wheel before testing. The two edges on the tensile surface were rounded with a radius about 0.15 mm in order to eliminate a failure initiated from an edge of the specimen. The specimens were tested in four point bending fixture (inner span of 20 mm and an outer span of 40 mm) with the crosshead

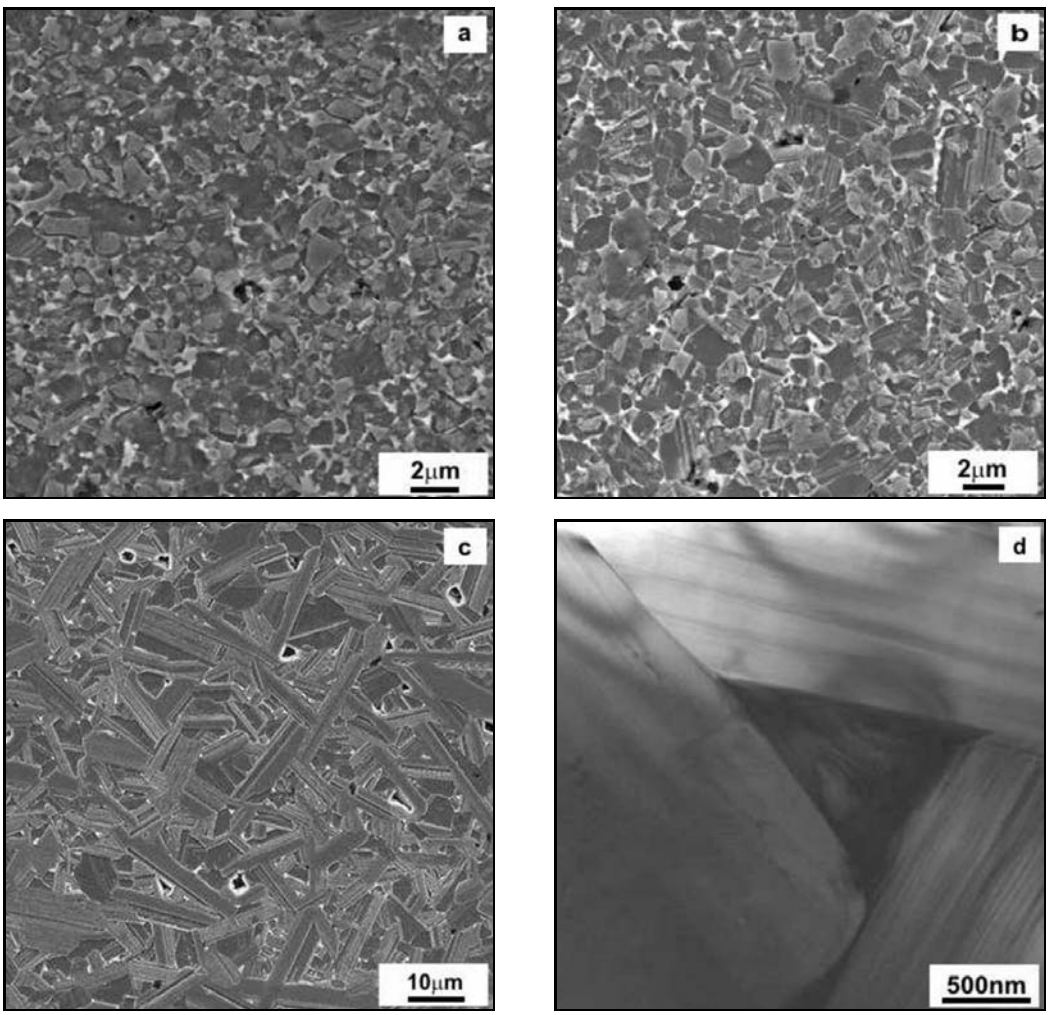

Fig. 1. SEM micrographs of SiC + Si_3N_4 composites: a) hot pressed at 1870 °C/1 h (SC-N-G5); b) HP + annealed at 1650 °C/5 h (SC-N-A5); c) HP + annealed at 1850 °C/5 h (SC-N-B5); d) TEM micrograph – triple point in SC-N-B5.

speed of 0.5 mm min^{-1} at ambient temperature and atmosphere. The characteristic flexural strength and Weibull modulus were computed using two-parameter Weibull distribution. Fractographic analysis of broken bend specimens was used to characterize the fracture origins, their location, size, shape and chemical composition.

3. Results and discussion

Figure 1 shows the characteristic microstructures of the sintered and annealed materials. The microstructures of hot pressed SC-N-G5 material (Fig. 1a) and SC-N-A5 composite annealed at 1650 °C (Fig. 1b) consist of fine submicron-sized equiaxed SiC grains with a low aspect ratio. No visible effect of the heat treatment at 1650 °C was found on the microstructure of the material. All the composites additionally contain intragranular phase in the form of a very thin grain boundary films and in the form of triple points with a size up to ca 0.5 μm (Fig. 1d). An average size of SiC grains in SC-N-A5 material is approximately 450 nm. The microstructure of SiC + Si_3N_4 composite is significantly changed after post-sintering high temperature treatment at 1850 °C (SC-N-B5, Fig. 1c). It consisted of elongated SiC grains with average size of 2.2 μm and with average length of 4.1 μm. The grain size distributions of the SiC grains in the systems SC--N-A5 and SC-N-B5 are illustrated in Fig. 2. The grain shape changed from almost globular to elongated; the mean aspect ratio increased from 1.1 for SiC + Si_3N_4 material as-received and annealed at 1650 °C to 4.4 for SiC + Si_3N_4 composite annealed at 1850 °C. Annealing at higher temperature and longer time results in the β-α transformation, which is accompanied by α grains growth and change of the grain shape.

Phase analysis of the hot pressed SC-N-G5 and annealed materials SC-N-A5 by XRD showed β-SiC as a major phase and α-SiC, $Y_3Al_2(AlO_4)_3$, and $Y_3Al_5O_{12}$ as minor phases. The intragranular phase is rich in elements originating from oxide additives, i.e. yttrium

Table 2. Properties of SiC + Si_3N_4 composites

Sample designation	Measured density (g cm^{-3})	Vickers hardness (GPa)*	Fracture toughness (MPa m$^{1/2}$)**	Young's modulus (GPa)	Flexural strength (MPa)
SC-N-G5	3.205	21.9 ± 0.6	3.5 ± 0.4	351.2	464.7
SC-N-A5	3.203	22.9 ± 0.7	2.8 ± 0.2	373.3	557.1
SC-N-B5	3.193	23.3 ± 0.4	4.4 ± 0.2	312.8	373.5

* Vickers hardness was measured at the applied load of 9.8 N. ** Fracture toughness was measured at the applied load of 98.1 N.

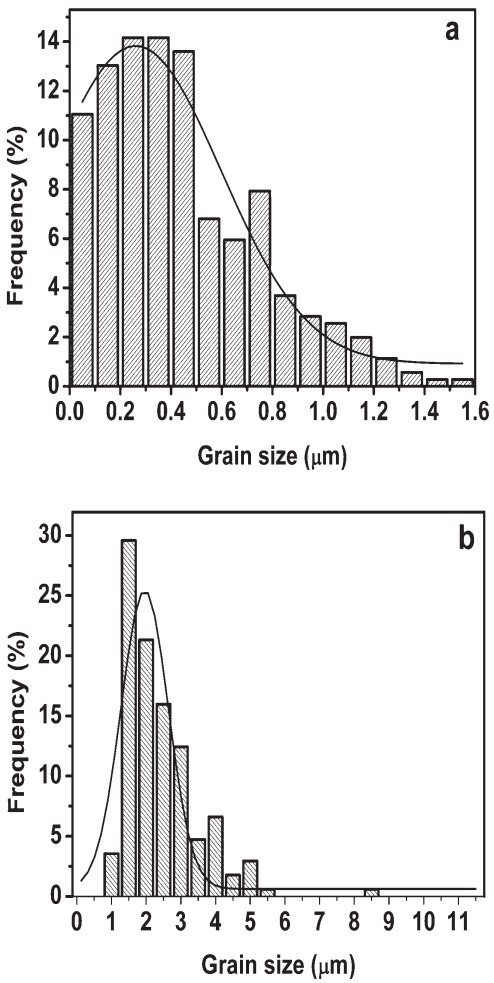

Fig. 2. Size distribution of the SiC particles in SiC + Si_3N_4 composites: a) HP + annealed at 1650 °C/5 h; b) HP + annealed at 1850 °C/5 h.

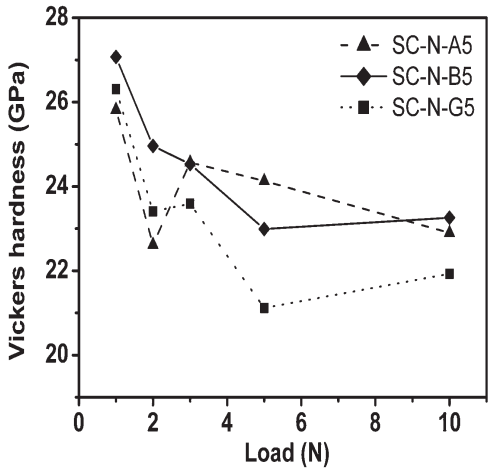

Fig. 3. Dependence of Vickers hardness on applied indentation load.

and aluminium. The SC-N-B5 composite contained α-SiC as a major phase. In SC-N-B5 material indications of β-α phase transformation during annealing is clearly visible.

The values of the Young's modulus are shown in the Table 2. For the composite, the Young's modulus can be estimated using the law of mixtures, $E = E_a V_a + E_b V_b$, where V_a and V_b are the volume fractions of the constituents. For investigated materials containing 5 % of Si_3N_4 with the modulus of elasticity 310 GPa [9] this equation gives $E = 395.5$ GPa. The composites exhibit lower values, however comparable to the used theoretically calculated value. As it is obvious from Fig. 3, microhardness shows a slight decrease when indentation load is increased. This load-size effect is in agreement with other investigations [25–27]. According to the results the material annealed at 1650 °C exhibits the highest Young's modulus. The reason of this behaviour are probably the changes introduced in the intragranular phase because the annealing has no influence on the grain size/shape. The fracture toughness values varied in range from 2.9 to 5.5 MPa m$^{1/2}$, Fig. 4. The heat treatment at 1650 °C caused a slight hardness improvement, on the other hand, however, a slight but evident toughness decrease. Because of the unchanged grain shape this can be explained only by changes in intragranular phase. These results revealed that, except for the system SC-N-B5, the composites do not exhibit rising fracture toughness with increasingindentation load. It is evident on the other side that the fracture toughness increased as the annealing temperature increased from 1650 °C to 1850 °C and the grain size increased from 450 nm to 2.2 μm. It is interesting to note, that the fracture toughness of this composite was found significantly higher only at the applied loads of 49.05

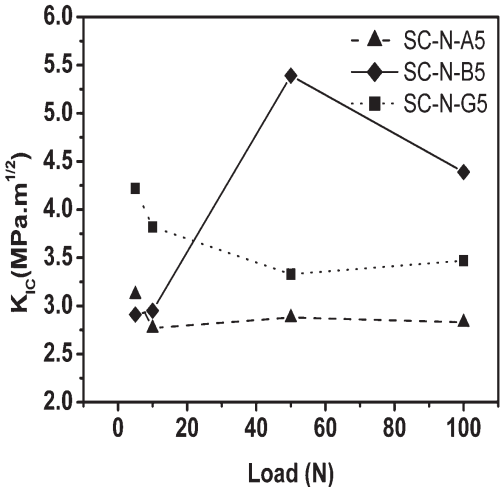

Fig. 4. Dependence of indentation fracture toughness on applied indentation load.

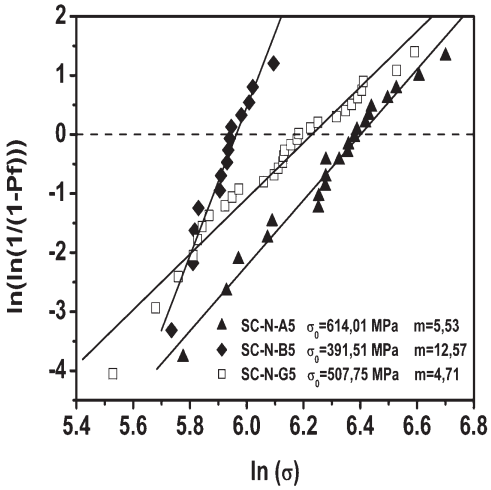

Fig. 5. Weibull plot of hot pressed and annealed SiC + Si_3N_4 composites.

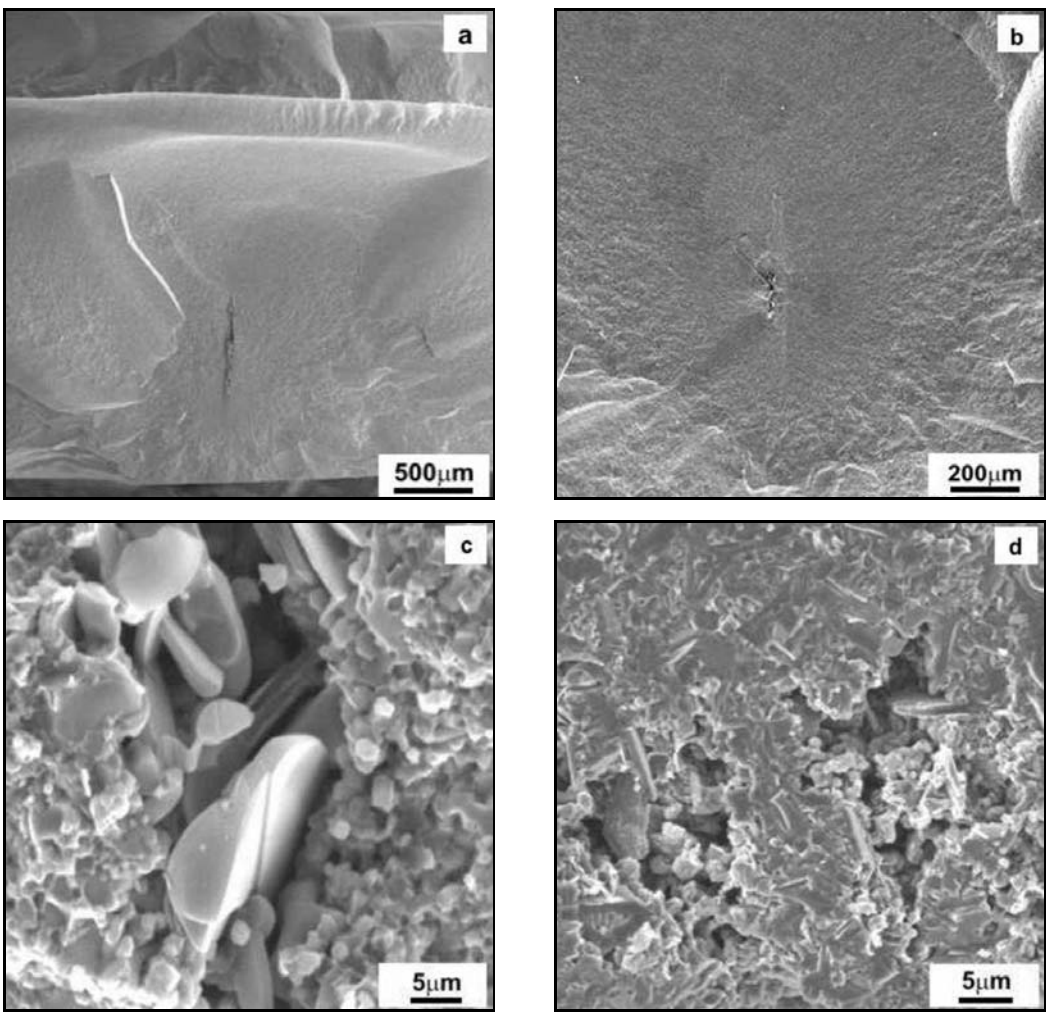

Fig. 6. SEM pictures of the typical fracture origins of SiC + Si_3N_4 composites: a) hot pressed; b), c) HP + annealed at 1650 °C/5 h; d) HP + annealed at 1850 °C/5 h.

and 98.1 N, i.e. when the crack length to indent size ratio was higher than 3.15.

Figure 5 shows the comparison of the characteristic flexural strength and Weibull modulus of the experimental materials. The material SC-N-A5 showed higher characteristic flexural strength (614 MPa) as hot pressed SC-N-G5 (507.8 MPa). The composite SC-N-B5 annealed at 1850 ℃/5 h possesses the lowest characteristic flexural strength $\sigma_0 = 391.5$ MPa and the highest Weibull modulus $m = 12.6$. The higher value of Weibull modulus of the specimens in the case of low characteristic strength indicates that defects with a similar size, geometry and location are responsible for the strength degradation. The Weibull modulus was significantly lower for materials SC-N--A5 and SC-N-G5. The low values of Weibull modulus suggest high scatter of flexural strength values. Macrofractographic observations have shown that the fracture origins are often at processing defects being mainly in the form of pores and clusters of pores (Fig. 6). The fracture initiation sites are located predominantly in the volume of the specimens, sometimes out from the tensile surface. The shape of the defects are different, there are crack-like pores, pores with irregular shape and clusters of pores. The size of fracture origins is lying in the interval from 40 μm to 200 μm. For the system SC-N-B5, processing flaws were found as the fracture origin, which causes the low characteristic flexural strength and relatively high Weibull modulus nearly in all specimens.

Microfractographic observations of the fracture surface and fracture profiles (Fig. 7) have shown that the crack propagation was controlled by mixed intra- and transgranular failure in all materials with slightly higher intragranular portion in the system annealed at 1850 ℃/h. The fracture profile in the as received and annealed composite at 1650 ℃/h is usually flat with a very low roughness. The roughness of the profile was significantly higher in the system annealed at 1850 ℃/5 h comparing to the as-received system. Crack deflection and crack bridging or crack branching were identified as the main toughening mechanisms in this material. Probably such toughening mechanisms are responsible for the higher fracture toughness. This is in agreement with published results. According to [28] the predominant toughening mechanism in SiC materials with oxide additives is a crack bridging. As reported by Do-Hyeong and Chong Hee [29], crack deflection is responsible for fracture toughness increasing in liquid-phase-sintered SiC.

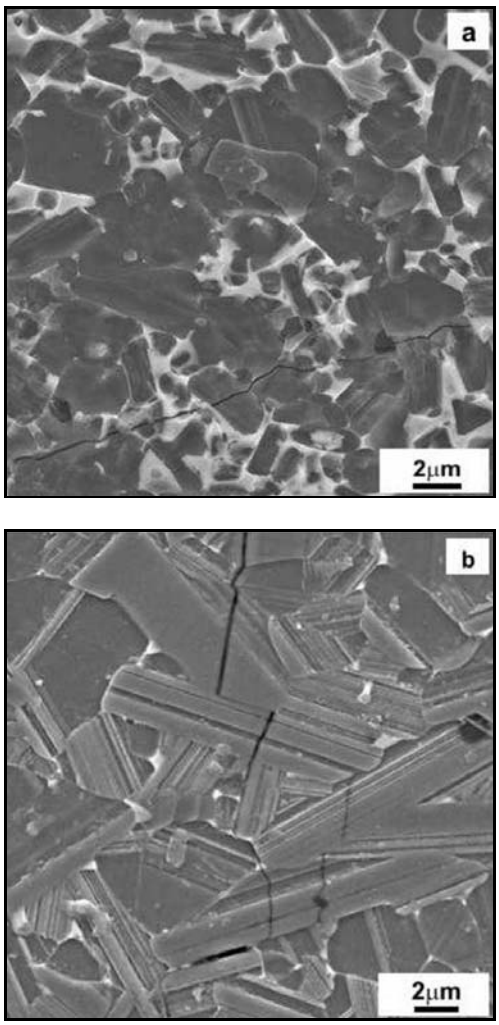

Fig. 7. SEM micrograph illustrating crack propagation in the materials: a) HP + annealed at 1650 ℃/5 h; b) HP + annealed at 1850 ℃/5 h.

4. Conclusion

The influence of the microstructure of liquid phase sintered and heat-treated SiC + Si_3N_4 composites on their mechanical properties, namely Young's modulus, Vickers hardness, indentation fracture toughness, and flexural strength was investigated. The main results are the following:

– In all SiC + Si_3N_4 composites a "load size effect" was found when testing their Vickers hardness. The microhardness values of the SiC + Si_3N_4 composites lying in the interval from 25.8 to 26.9 GPa and the Young's modulus varied from 312.8 to 373.3 GPa;

– The indentation fracture toughness values were in the interval from 2.9 to 5.5 MPa $m^{1/2}$, the highest values were identified for material annealed at 1850 ℃/5 h (SC-N-B5). Crack deflection, crack bridging and crack branching as the main toughening mechanisms are responsible for the toughness improvement;

– The characteristic strength values are relatively low and changing from 391.5 to 614 MPa with Weibull modulus from 4.7 to 12.6. The strength values are degraded by processing flaws present in the investigated

materials having different size from 40 μm to 200 μm. After eliminating these defects significant strength improvement can be expected.

Acknowledgements

The paper was supported by the Slovak Grant Agency via No. 2/7194/27, by Nanosmart, Centre of Excellence of SAS, by Marie Curie Host Fellowships under contract No. HPMT-CT-2001-00372, and by KMM-NoE project of the EU 6FP.

References

[1] FALK, K. L.: J. Eur. Ceram. Soc., *69*, 1997, p. 983.
[2] PROCHAZKA, S.: In: Proceedings of the Conference on Ceramics for High Performance Applications. Eds.: Burke, J. E., Gorum, A. E., Katz, R. N. Chestnut Hill, MA, Brook Hill Publ. Co. 1975, p. 239.
[3] PADTURE, N. P.: J. Am. Ceram. Soc., *77*, 1994, p. 519.
[4] MULLA, M. A.—KRSTIC, V. D.: J. Mater. Sci., *29*, 1994, p. 34.
[5] OMORI, M.—TAKEI, H.: J. Am. Ceram. Soc., *65*, 1982, C-92.
[6] SIGL, L. S.—KLEEBE, H. J.: J. Am. Ceram. Soc., *76*, 1993, p. 773.
[7] KEPPELER, M.—REICHERT, H. G.—BROADLEY, J. M.—THURN, G.—WIEDMANN, I.—ALDINGER, F.: J. Eur. Ceram. Soc., 18, 1998, p. 521.
[8] NADER, M.—ALDINGER, F.—HOFFMANN, M. J.: J. Mater. Sci., *34*, 1999, p. 1197.
[9] GONDÁR, E.—GÁBRIŠOVÁ, Z.—ROŠKO, M.—ZEMÁNKOVÁ, M.: Kovove Mater., *44*, 2006, p. 113.
[10] CAO, J. J.—MOBERLYCHAN, W. J.—DE JONGHE, L. C.—GILBERT, C. J.—RITCHIE, R. O.: J. Am. Ceram. Soc., *79*, 1996, p. 461.
[11] TANAKA, H.—ZHOU, U.: J. Mater. Res., *14*, 1999, p. 518.
[12] MULLA, M. A.—KRSTIC, V. D.: Acta Metall. Mater., *42*, 1994, p. 303.
[13] LEE, S. K.—KIM, C. H.: J. Am. Ceram. Soc., *77*, 1994, p. 1655.
[14] KIM, Y. W.—MITOMO, M.—HIROTSURU, H.: J. Am. Ceram. Soc., *78*, 1995, p. 3145.
[15] ZHAN, G. D.—MITOMO, M.—KIM, Y. W.: J. Am. Ceram. Soc., *82*, 1999, p. 2924.
[16] PADTURE, N. P.—LAWN, B. R.: J. Am. Ceram. Soc., *77*, 1994, p. 2518.
[17] SHINOZAKI, S. S.—HANGAS, J.—CARDUNER, K. R.—ROKOSZ, M. J.—SUZUKI, K.—SHINOHARA, N.: J. Mater. Res., *8*, 1993, p. 1635.
[18] ZHAN, G. D.—XIE, R. J.—MITOMO, M.—KIM, Y. W.: J. Am. Ceram. Soc., *84*, 2001, p. 945.
[19] ZHOU, Y.—HIRAO, K.—YAMAUCHI, Y.—KANZAKI, S.: J. Eur. Ceram. Soc., *22*, 2002, p. 2689.
[20] RIXECKER, G.—WIEDMANN, I.—ROSINUS, A.—ALDINGER, F.: J. Eur. Ceram. Soc., *12*, 2001, p. 1013.
[21] SCITI, D.—BELLOSI, A.: J. Mater. Sci., *35*, 2000, p. 3849.
[22] CHOI, H. J.—KIM, Y. W.—MITOMO, M.—NISHIMURA, T.—LEE, J. H.—KIM, D. Y.: Scripta Mater., *50*, 2004, p. 1203.
[23] KIM, Y. W.—CHUN, Y. S.—NISHIMURA, T.—MITOMO, M.—LEE, Y. H.: Acta Mater., *55*, 2007, p. 727.
[24] ANSTIS, G. R. et al.: J. Am. Ceram. Soc., *64*, 1981, p. 533.
[25] LI, H.—GOSH, A.—HAN, Y. H.—BRADT, R. C.: J. Mater. Res., *8*, 1993, p. 1028.
[26] IOST, A.—BIGOT, R.: J. Mater. Sci., *31*, 1996, p. 3573.
[27] PENG, Z.—GONG, J.—MIAO, H.: J. Eur. Ceram. Soc., *24*, 2004, p. 2193.
[28] PADTURE, N. P.: J. Am. Ceram. Soc., *77*, 1994, p. 519.
[29] DO-HYEONG, K.—HEE CHONG, K.: J. Am. Ceram. Soc., *73*, 1990, p. 1431.